Columbia University — Department Of Chemical Engineering
ENGINEERING RESEARCH LABORATORIES

TOPICAL REPORT # 2

TASK XV OF CONTRACT AT(30-3)-187

MASTER

HEAT TRANSFER AND HYDRAULIC STUDIES FOR SNAP-4 FUEL ELEMENT GEOMETRIES

September, 1963

Bruce Matzner

TID-19563

Introduction

Task XV is concerned with the evaluation of the thermal and hydraulic characteristics of a high performance boiling water nuclear reactor being developed by Atomics International. This reactor has a core which amounts to an almost infinite array of short (17" length), closely spaced fuel rods. It is being simulated in the Task XIII high pressure boiling water loop by a wire-wrapped 12-rod bundle in vertical upflow at 1200 psia.

1. Summary

(42) instrumented burnout points were obtained with the second 12-Rod Test Section which was geometrically almost identical to the first 12-Rod Test Section. Considerable pressure drop and heat transfer data were also taken. The ranges of variables studied were: mass velocities from 0.5 to 4.1 x 10^6 lb/hr-ft^2, exit qualities between 2 and 52% and instrumented burnout heat fluxes as high as 1.28 x 10^6 Btu/hr-ft^2.

For all but 3 of the burnout runs temperature instabilities originated on one of the obtuse corner rods. Because there is evidence to show the flow area was smaller around this obtuse corner rod than around the other outer rods the burnout data for this experiment should be considered a conservative estimate of the burnout performance of this geometry.

2. Test Section Description

The test section consisted of (12) 347 stainless steel rods

DISCLAIMER

having a 0.440" O.D. and a 17" heated length. All the rods were wrapped with hypodermic needle tubing of 0.022" O.D. on a 6" pitch. The rods were arranged with a triangular pitch in three rows of 4 rods each to form a 60° parallelogram (Figure 1). The center to center distance between all adjacent rods was 0.4625". The minimum distance from any outer rod to the asbestos-phenolic shroud wall was maintained by the wire wrap. The flow area was 0.471 sq. in. and the hydraulic diameter was 0.079".

3. Instrumentation

All (12) rods were fitted with voltage taps so that they could be monitored by a resistance bridge burnout detector. Six of the rods (Nos. 2,4,5,7,9, and 11) were equipped with iron-constantan thermocouples located at the downstream end of the heated length. Unless the burnout detector signals were very strong, conditions of incipient burnout were considered to have occurred only after a transient temperature rise was indicated on one of the rod thermocouples.

Test section flow rates were measured by a 7/8" Potter turbine flow meter and test section pressure drops by a 60" mercury manometer.

4. Test Results

4.1 Burnout Data

Forty-two instrumented (incipient) burnout points were obtained with the second 12-Rod Test Section (Table 1). The last five of these runs were carried somewhat beyond incipient burnout to where a rod surface temperature had risen about 90°F. The ranges of variables covered were:

Mass velocity: 0.5 to 4.1 x 10^6 lb/hr-ft^2

Burnout heat flux: 0.27 to 1.28 x 10^6 Btu/hr-ft^2

Exit steam quality: 2 to 52%

At the conclusion of these runs the test section was removed from the loop in practically undamaged condition.

4.1.1 Comparison of the Burnout Data for Test Sections # 1 and # 2

Test sections # 1 and # 2 were geometrically identical except for one detail. The position of the wire wraps of the heater rods were rotated 180°. The most important difference between the two sections was in their thermocouple instrumentation. The six rod thermocouples installed in the first test section were placed at different axial locations which were appropriate for gathering heat transfer information but did not contribute to supplying burnout protection. Therefore, the resistance bridge burnout detector was in reality the sole burnout indicator. In the second test section the six rod thermocouples were placed at the downstream end of the rods where they could effectively be employed as burnout indicators. Hence, the burnout data from the second test section should be considered to be more accurate.

To determine the reproducibility of the burnout data obtained from both test sections an attempt was made to reproduce the best established point from the first test section. This undoubtedly was Run 21 which culminated in a physical burnout. This was done successfully by Run 58 in which an instrumented burnout point was obtained at a slightly lower heat flux and exit quality than Run 21 while operating at essentially the same inlet fluid conditions.

4.1.2 The Effect of Mass Velocity on Burnout

The burnout data show a strong direct mass velocity effect (i.e. burnout heat flux increases with mass velocity for a constant exit quality) in the low quality region (Figure 2). This is characteristic of the bubble flow regime. As the exit quality is increased an inverse mass velocity effect is evident. This is characteristic of the fog flow regime.

In the direct mass velocity region the burnout data show a surprisingly small variation in burnout heat flux for relatively large changes in exit quality especially at the lower mass velocities. Two possible explanation for this effect are:

1. The local steam quality at the burnout location is not changing as rapidly as the bulk average quality.

2. A new, previously unobserved, mechanism is responsible for the local burnout.

4.1.3 Burnout Location and the Unheated Wall Effect

On all but three of the 42 burnout runs the primary burnout indication came from Rod # 4, one of the obtuse corner rods. On disassembly the only overheated areas were on the downstream ends of Rods 4, 8, and 12 facing the housing wall. Of these three only Rod # 4 showed a significant area of overheating (about 2" long). No evidence of overheating was found on the upstream end of Rod # 4 where a physical burnout had occurred with the first test section.

The incidence of nearly all the instrumented burnouts on one of the obtuse corner rods brings up the following question. Is the lower burnout performance of Rod # 4 typical of the other rods in the test section and thus causing an unnecessarily pessimistic evaluation of this geometry? Experiments with internally and doubly heated annuli (Ref. 1) have shown that a heating surface facing an unheated wall will have a lower burnout heat flux, for the same local quality and mass velocity, than the same heating surface when it faces a heated wall. Unfortunately there are no experiments reported in the literature which would allow an exact evaluation of the detrimental effect of an unheated wall. Even if such information were available our knowledge of the local quality and mass velocity would not be sufficient to use it.

From observations made during the running of this experiment there is good reason to believe that the mass velocity in the channel between Rod # 4 and the housing wall was considerably lower than the bulk average. The thermocouple on Rod # 4 which faced the unheated housing wall repeatedly indicated subcooled boiling conditions while the five other rod thermocouples (at the same axial position) indicated heat was still being transferred by single phase forced convection in the rest of the bundle. From this it can be concluded that the local single phase forced convection heat transfer coefficient at the Rod # 4 thermocouple was considerably lower than at the five other rod thermocouples. This in turn leads to the conclusion that the local liquid velocity in the channel between Rod # 4 and the housing wall was lower than the average liquid velocity. If this effect persisted into the bulk boiling region the local burnout heat flux for Rod # 4 would be reduced relative to the other rods in the bundle.

There is evidence that the gap between Rod # 4 and the housing wall was closer than for other outer rods in the bundle. Slight indentations ($\simeq$ 2 mils deep) made by the wraps of Rod # 4 in the asbestos-phenolic housing wall were found on disassembly of the test section. This explains why the velocity at this location was reduced and also why burnout was not detected on the other obtuse corner rod. Undoubtedly, even if the flow was perfectly distributed around the outer rods, one of them would have reached burnout before either of the two inner rods due to the unheated wall effect.

4.1.4 Effect on Burnout of the Gap Size Between the Outer Rods and the Flow Channel Wall

Elaborate care was taken in the design of this experiment to minimize the free flow area between the outer rods and the housing wall. Burnout experiments at 1200 psig on closely spaced wire wrapped 19-rod bundles where the gap between the outer rods and the housing wall was greater than the minimum rod spacing, were carried out at the Hanford Laboratories (Ref. 2). The following two uniformly heated Hanford 19-rod test sections are of interest to this discussion:

Hanford Test Section Number	Spacing Between Rods Within Bundle	Nominal Spacing Between Outer Rods and Pressure Tube	Heater Rod O.D.	Heater Length	Wire Wrap Diam.	Wire Wrap Pitch
II	0.015"	0.060"	0.629"	19.5"	0.015"	10"
IV	0.050"	0.101"	0.587"	19.5"	0.050"	9"

Comparing the data of the 12-rod test sections with the Hanford 19-rod data (Figure 3) shows that all the 12-rod burnout data are higher than the 19-rod data for the test section with 15 mil rod spacing. The 12-rod burnout data are also as high or higher than the 19-rod data for the test section with 50 mil rod spacing. These comparisons demonstrate that at least one other variable besides the minimum rod spacing must be considered when analyzing rod bundle burnout.

The most significant variable might be the spacing between outer rods and the housing wall. In the Hanford tests where a relatively large gap existed between the outer rods and the housing wall, burnout invariably occurred on the inner rods. This was caused by flow starvation of the inner rods. With the 12-Rod Test Sections, where no such gap existed, burnout occurred only on the outer rods. This was due to a combination of the unheated wall effect and flow starvation around outer Rod # 4.

4.1.5 Operation Beyond Incipient Burnout

Five runs were carried somewhat beyond incipient burnout to where a rod surface temperature (in all cases Rod # 4) had risen about 90°F (Table 2). The purpose of these runs was to determine how close to failure were the instrumented burnout runs. The temperature rises which were observed on Rod # 4 were quite sharp and were accomplished by very slight increase in heat flux (< 2%). They were characteristic of the fast temperature increases observed during nucleate boiling burnouts. From these runs it is estimated that the instrumented burnout heat fluxes are about 5% below the actual physical failure point.

4.1.6 Burnout Detector Operation Around 0% Exit Quality

During the burnout testing of the second 12-Rod Test Section on several occasions severe burnout detector fluctuations were encountered in the area of 0% exit quality. During Runs 33 and 50 these fluctuations were at first thought to be real burnout signals. Later it was observed that these fluctuations would weaken and disappear upon raising the heat flux without any rod temperature increases being observed. If the burnout detector had been the sole burnout indicator in this experiment several erroneously low burnout points would have been obtained.

Other experimenters who have reported reduced burnout heat fluxes in the region of 0% quality using only a resistance bridge burnout detector may have encountered the above effect.

4.1.7 Effect of Nitrogen Gas Bubbled in the Coolant Stream

After the completion of Run PD3 a large quantity of nitrogen gas was inadvertently introduced into the flow stream from the gas pressurizer. This caused oscillations in the measured flow rate of $\pm$ 10%. The heat flux during this period of operation was 1.05×10^6 Btu/hr-ft^2 with an exit quality of 0.9%. The system operated under these conditions for about three minutes with no indication of rod temperature instabilities. Later it was determined that at essentially the same inlet fluid conditions burnout occurred at a heat flux of 1.175×10^6 Btu/hr-ft^2 and an exit quality of 3.6%. This chance incident showed that the burnout heat flux for this test section was not overly sensitive to the presence of gas bubbles in the coolant stream even though the flow rate was affected.

4.2 Heat Transfer Data

Surface temperatures and heat transfer coefficients were calculated from the measured inside wall temperatures taken throughout the running period (Table 5). The following general observations were made from these data:

1. The non-burnout heat transfer coefficients generally ranged between 20,000 and 30,000 Btu/hr-ft^2 $^{\circ}$F.

2. It appeared that the boiling heat transfer coefficients increased somewhat with increasing mass velocity.

3. At low mass velocities the calculated rod surface temperatures from rod to rod were fairly non-uniform. At high mass velocities, however, the calculated rod surface temperatures were almost identical.

4.3 Pressure Drop Data

Seventeen separate pressure drop runs were made under non-burnout conditions (Table 4). Most of these runs were taken at constant rod heat fluxes of 600,000 , 500,000 and 400,000 Btu/hr-ft^2 so as to be able to plot total pressure over a 20" test section length versus volumetric flow rate (Figure 4). This plot shows that at an inlet temperature of 540°F and the above rod heat fluxes the flow through the test section is inherently stable.

Close inspection of the pressure drop data will show inconsistencies in the readings between various sets of pressure taps. These inconsistencies may be real errors in the pressure drop measurements or may be actual variations of the local pressure due to close proximity of the pressure tap holes to a turbulence promoting wire wrap. A good method which can be used to smooth any of these errors is to plot pressure profiles along the length of the test section.

The single phase friction pressure drop taken at room temperature with no heat input was observed to be slightly higherfor this test section than for the first 12-Rod Test Section (Figure 5).

5. Conclusions

5.1 A Qualitative Analysis of Burnout in a Rod Bundle

The basic assumption in this analysis is that there are two kinds of boiling heat transfer surface in the ordinary rod bundle geometry. The first kind is represented by an inner rod which is completely surrounded by other heat generating rods. The second kind is represented by an outer rod which is partially surrounded by other heat generating rods but also faces an unheated wall. Under identical conditions of mass velocity and local steam quality the outer rod surface which faces an unheated wall will have a lower burnout heat flux than the inner rod.

Maximum power will be extracted from a bundle with uniform heat generation when the burnout heat flux is equal on both kinds of heat transfer surfaces. For this to be possible a slightly greater flow rate would be necessary in the gap between the outer rods and the unheated walls than in the interior of the bundle. This is based on the assumption that at constant inlet temperature and heat flux raising the flow always provides a higher burnout safety factor. This could be accomplished by increasing the free flow area between the outer rods and the unheated walls.

It probably would be possible to increase the burnout heat flux of a particular rod bundle by providing a heated wall. Unfortunately this solution may not be feasible in a practical nuclear fuel element.

This analysis has neglected the effect on burnout heat flux of other geometrical variables such as rod diameter, minimum rod spacing and wire wrap pitch. At present there are insufficient data to permit an evaluation of the effect of any of these variables.

5.1.2 Results of this Experiment

The burnout data of this experiment represent the case where burnout was occurring on the outer rods due to a combination of the cold wall effect and insufficient flow area. The burnout performance of Rod No.4 where there was evidence to show the flow area was a minimum should have been somewhat higher. The results of this experiment therefore should provide conservative estimates of the burnout performance of the outer rods of the Snap-4 fuel element geometry.

6. Future Program

The immediate future program will be directed toward obtaining an estimate of the burnout heat flux of an inner rod as opposed to the burnout data already obtained for an outer rod facing an unheated wall. This will be achieved in the third 12-Rod Test Section by replacing the two normal inner rods with high powered rods which will generate approximately 2.5 times the heat flux of the other ten rods.

References

1. K. M. Becker & G. Hernborg, "Measurements of Burnout Conditions for Flow of Boiling Water in a Vertical Annulus" ASME Paper No. 63-HT-25, August, 1963.

2. E. D. Waters, G. M. Hesson, D. E. Fitzsimmons & J. M. Batch "Boiling Burnout Experiments with 19-Rod Bundles in Axial Flow", Report HW-77303, August, 1963.

CROSS SECTION OF SECOND 12 ROD TEST

SECTION AT 1/2" FROM EXIT END OF HEATED LENGTH

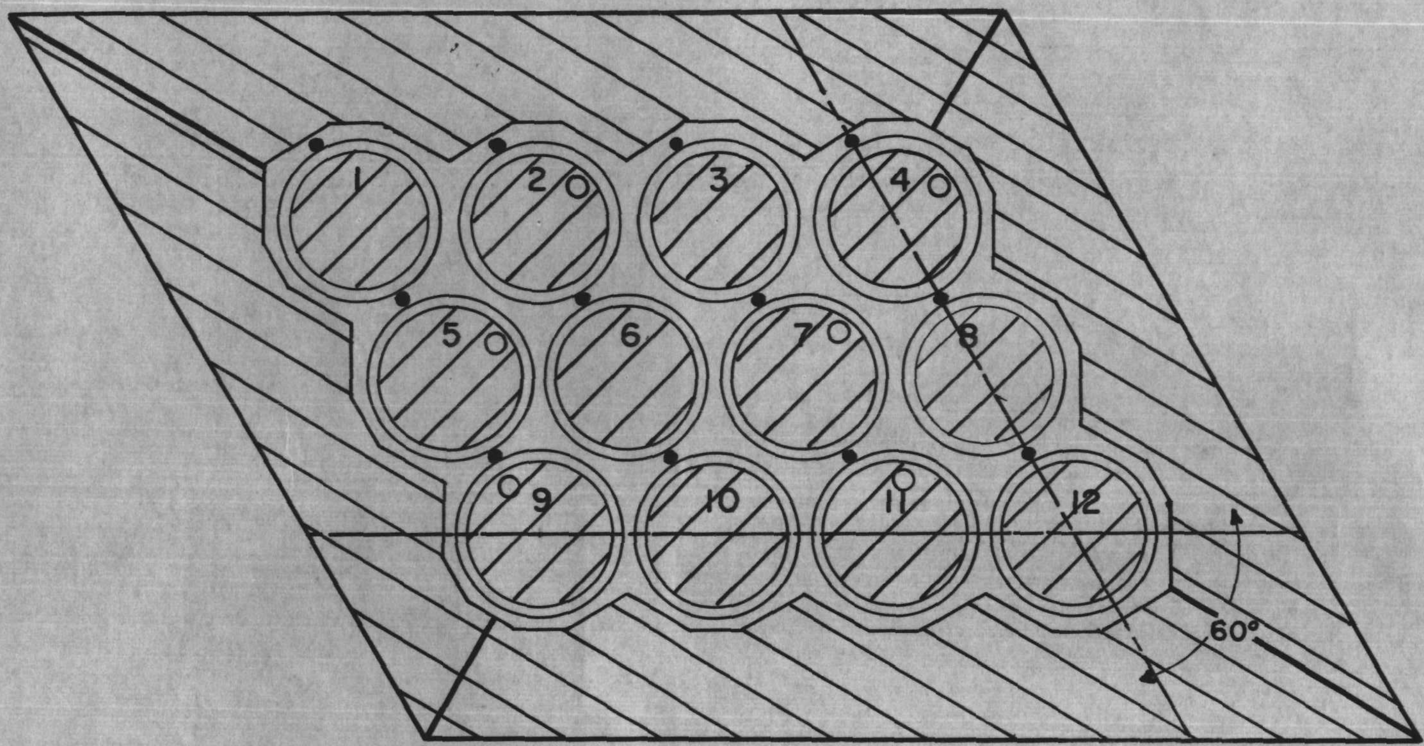

●= 12 TUBE WRAPS
OD.= 0.022

12 HEATER TUBES
OD.= 0.440

O= 6 THERMOCOUPLES

NOTE:

CENTER TO CENTER DISTANCE OF ALL ADJACENT TUBES IS 0.4625."

Figure 1

INSTRUMENTED BURNOUT HEAT FLUX VS. EXIT QUAL

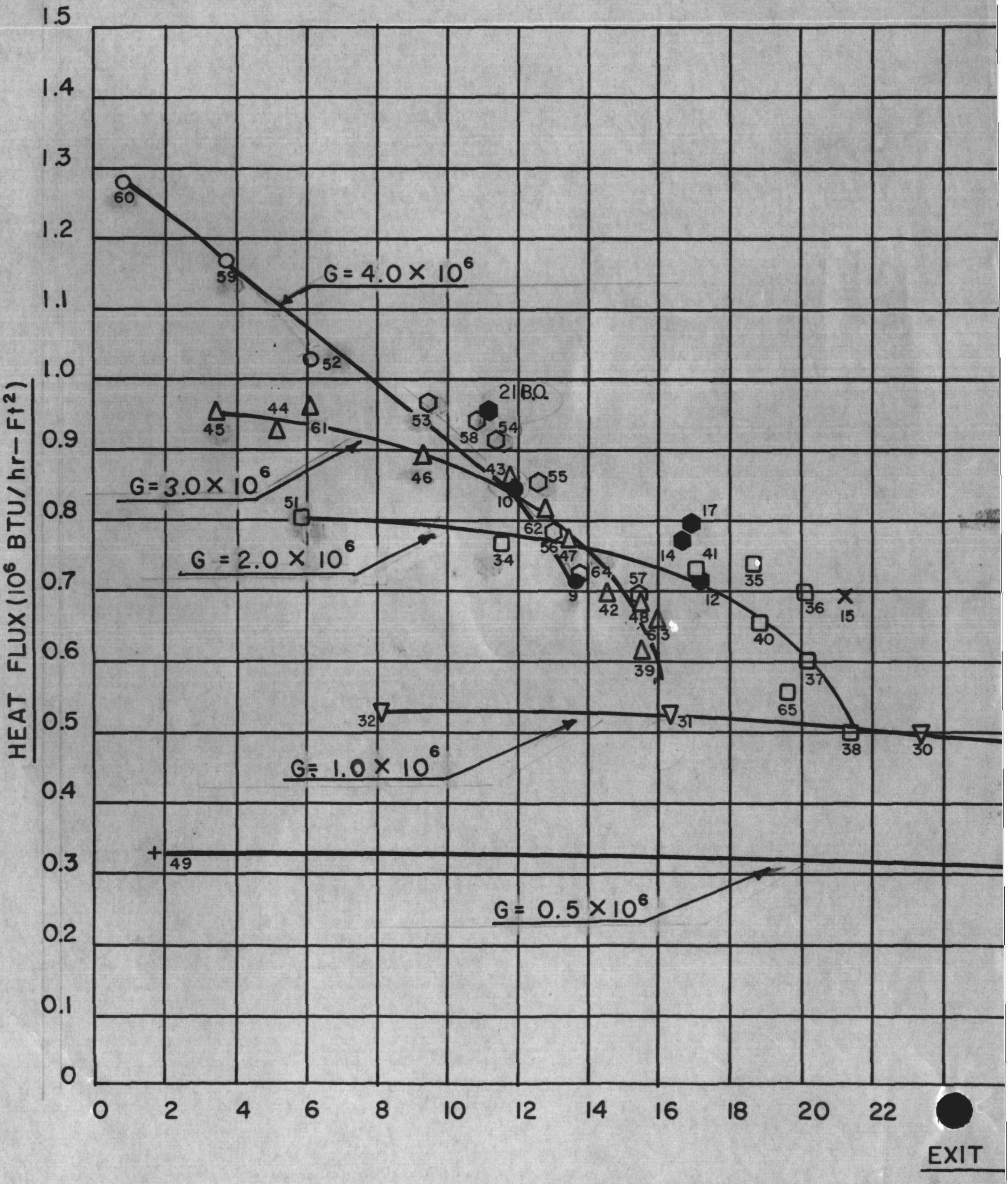

ITY FOR 12—ROD TEST SECTION

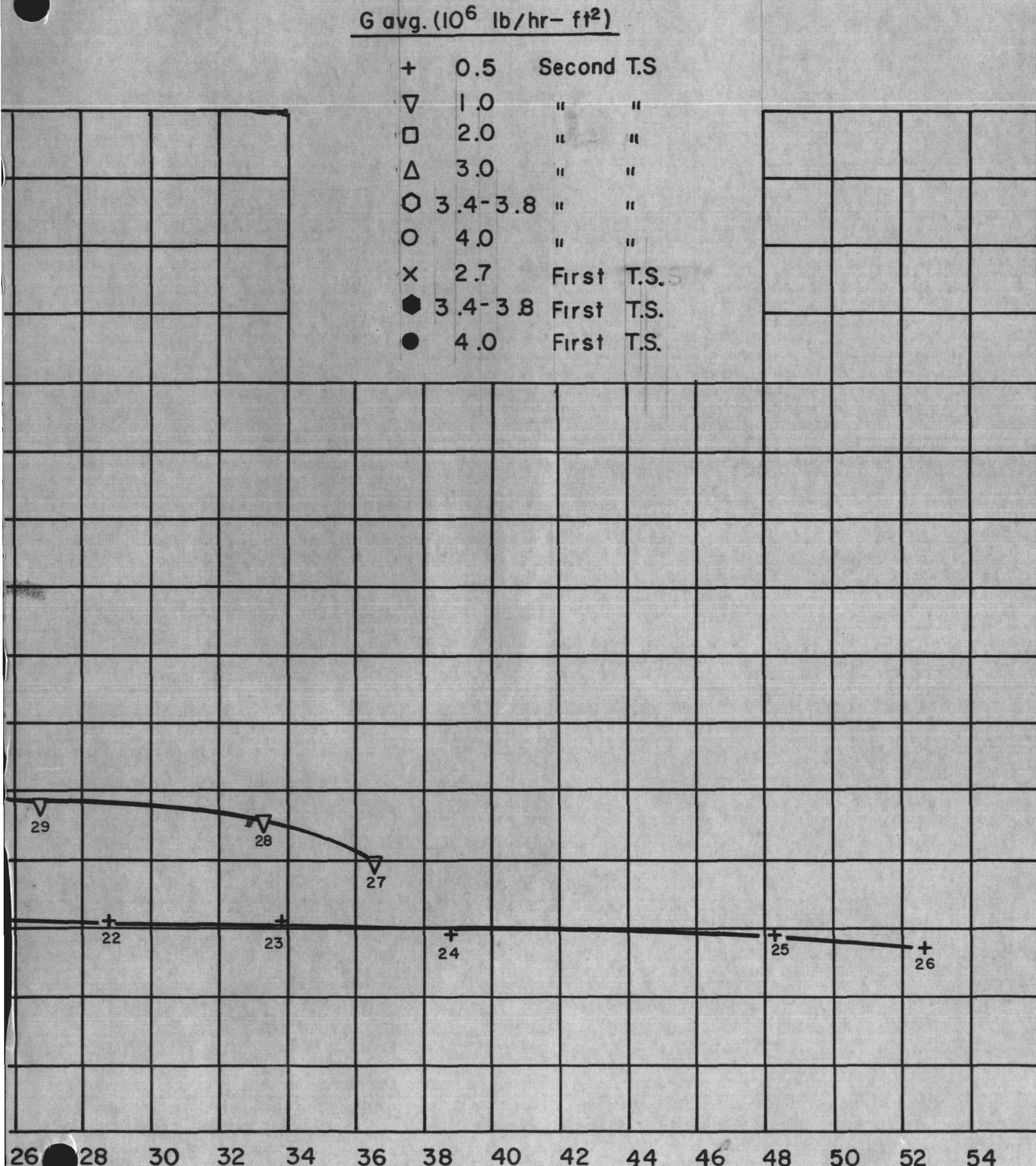

QUALITY (%)

Figure 2

COMPARISON OF 12 ROD TEST SECTION BURNOUT DATA WITH

HANFORD TEST SECTION NO. II
0.629" ROD O.D.; 0.015" MINIMUM ROD SPACING
HANFORD TEST SECTION NO. IV
0.587" ROD OD.; 0.050" MINIMUM ROD SPACING.

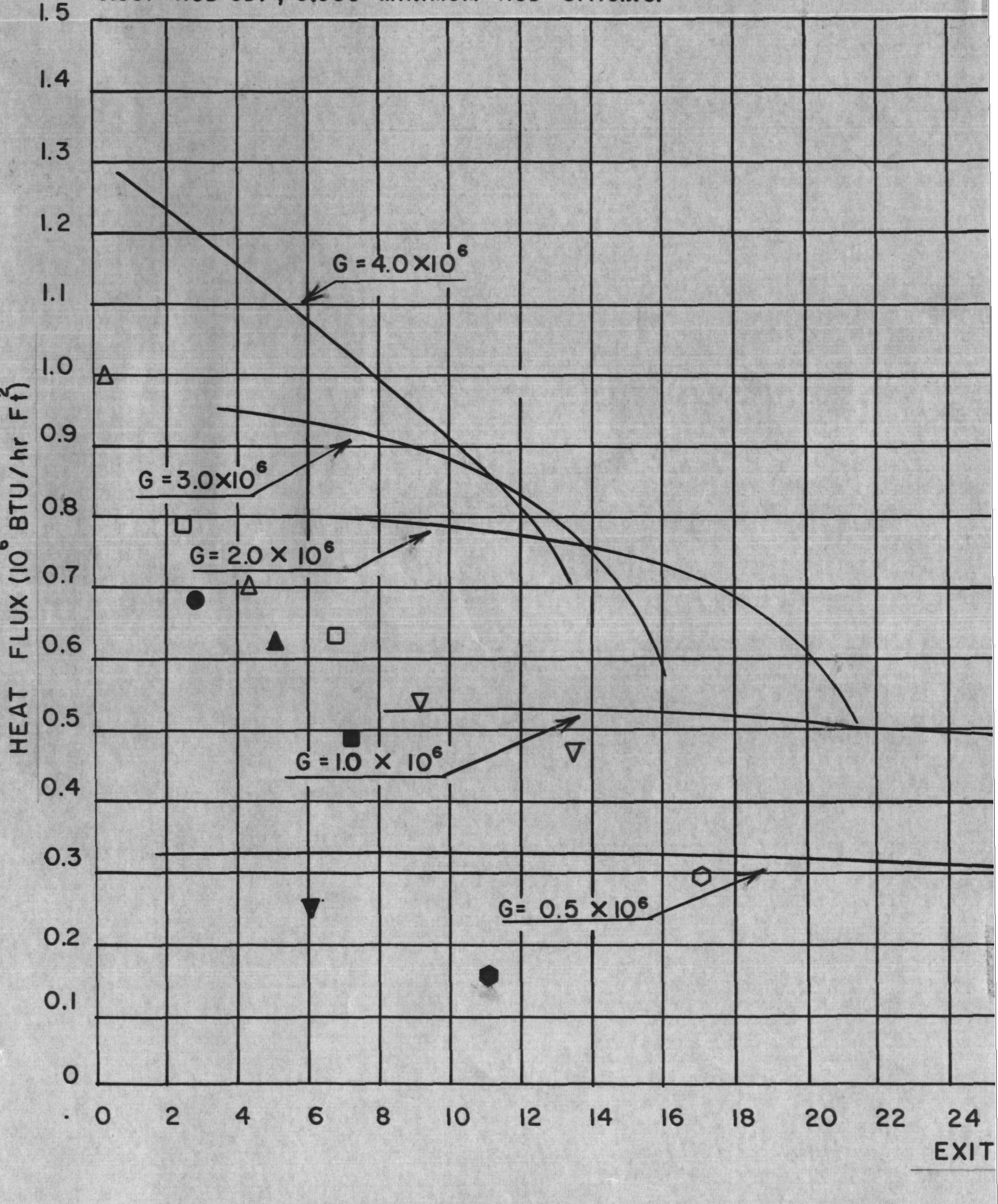

19 ROD BOUNDLE BURNOUT DATA FROM HANFORD.

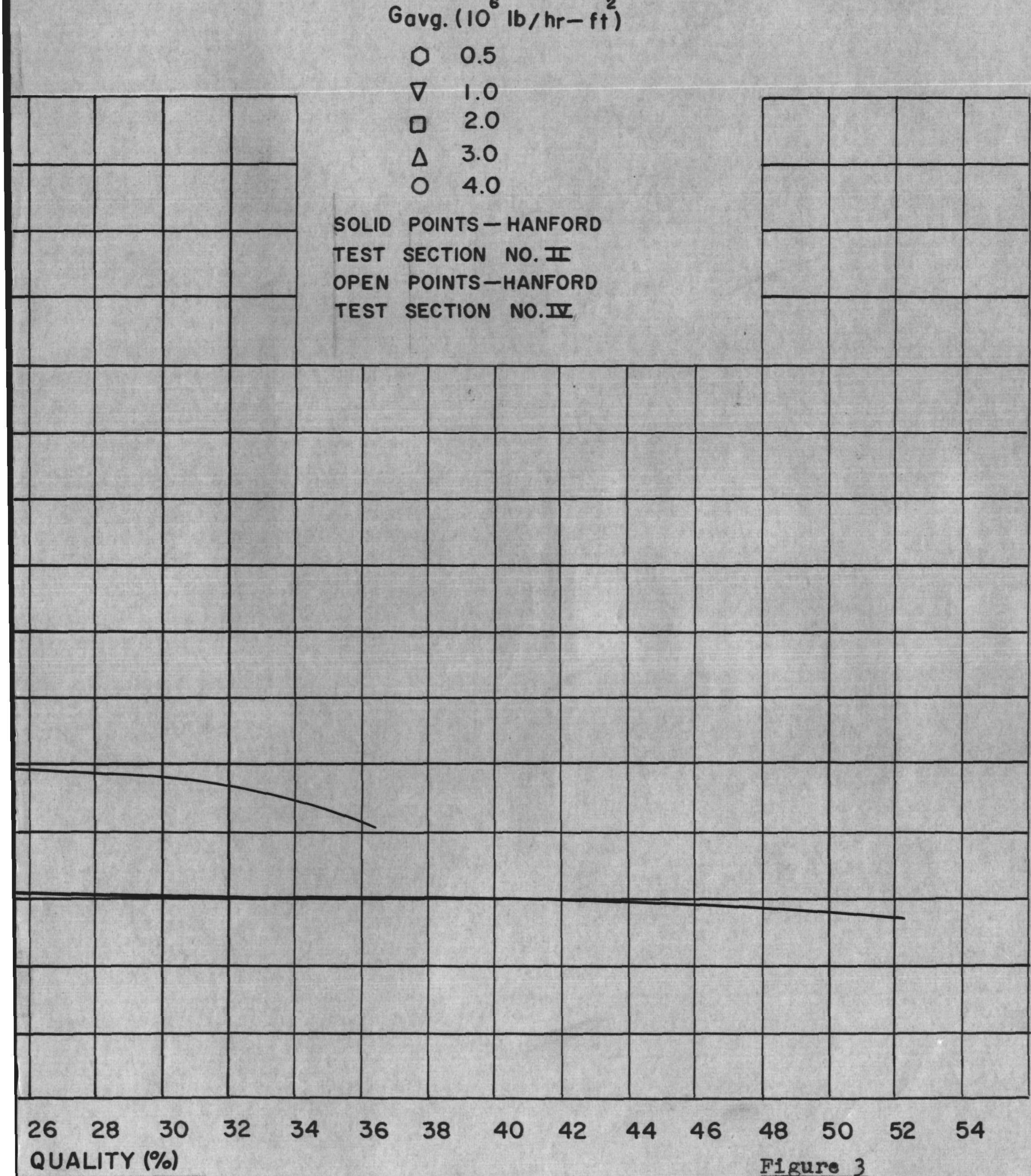

Figure 3

FRICTION PRESSURE DROP VS. FLOW FOR FIRST AND SECOND 12-ROD TEST SECTIONS. NO HEAT ADDITION P=1200 PSIA

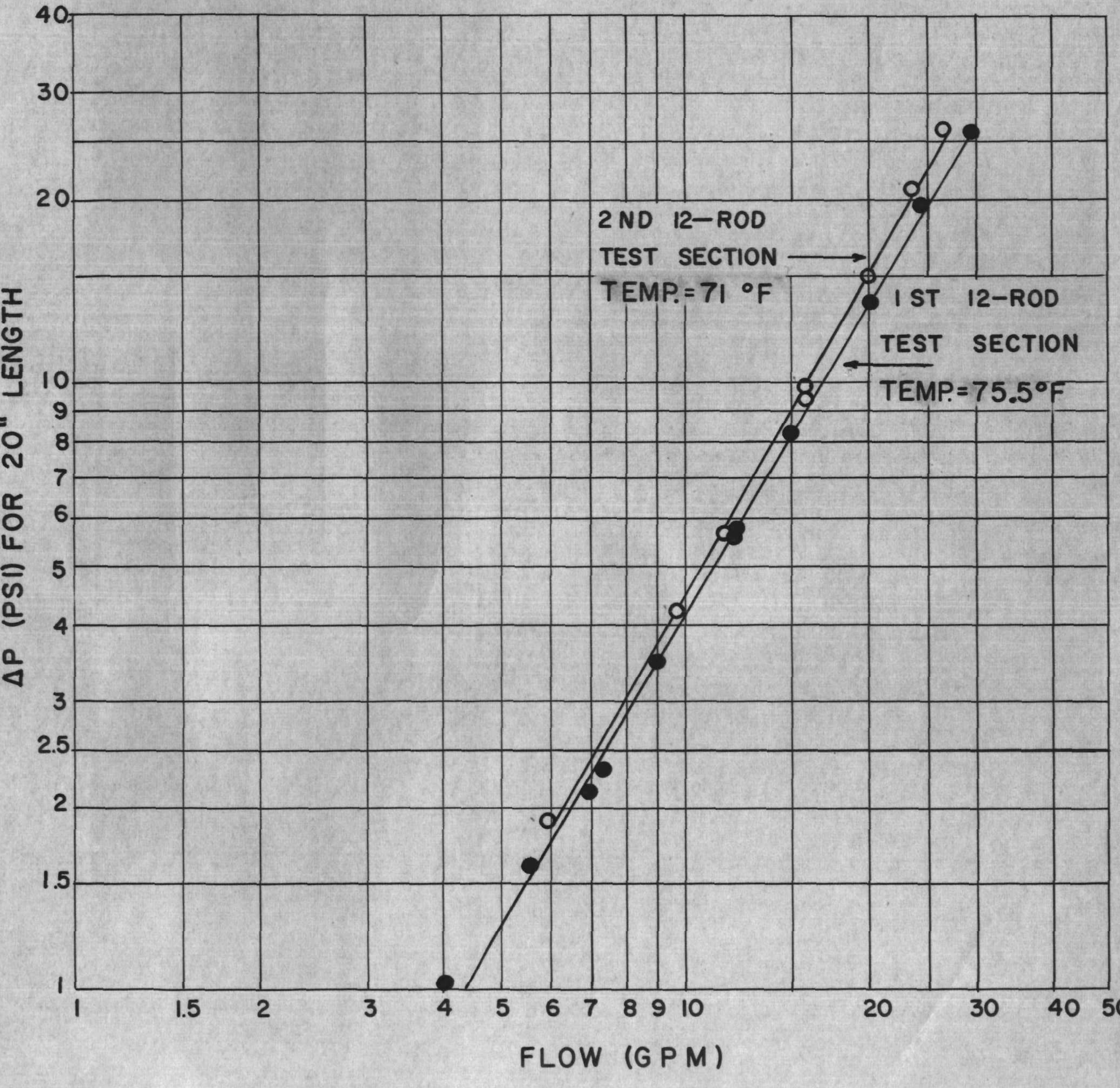

Figure 4

2^{nd} 12 ROD TEST SECTION

PRESSURE DROP VS. FLOW AT VARIOUS ROD HEAT FLUXES FOR CONSTANT INLET TEMP. OF 540 °F.

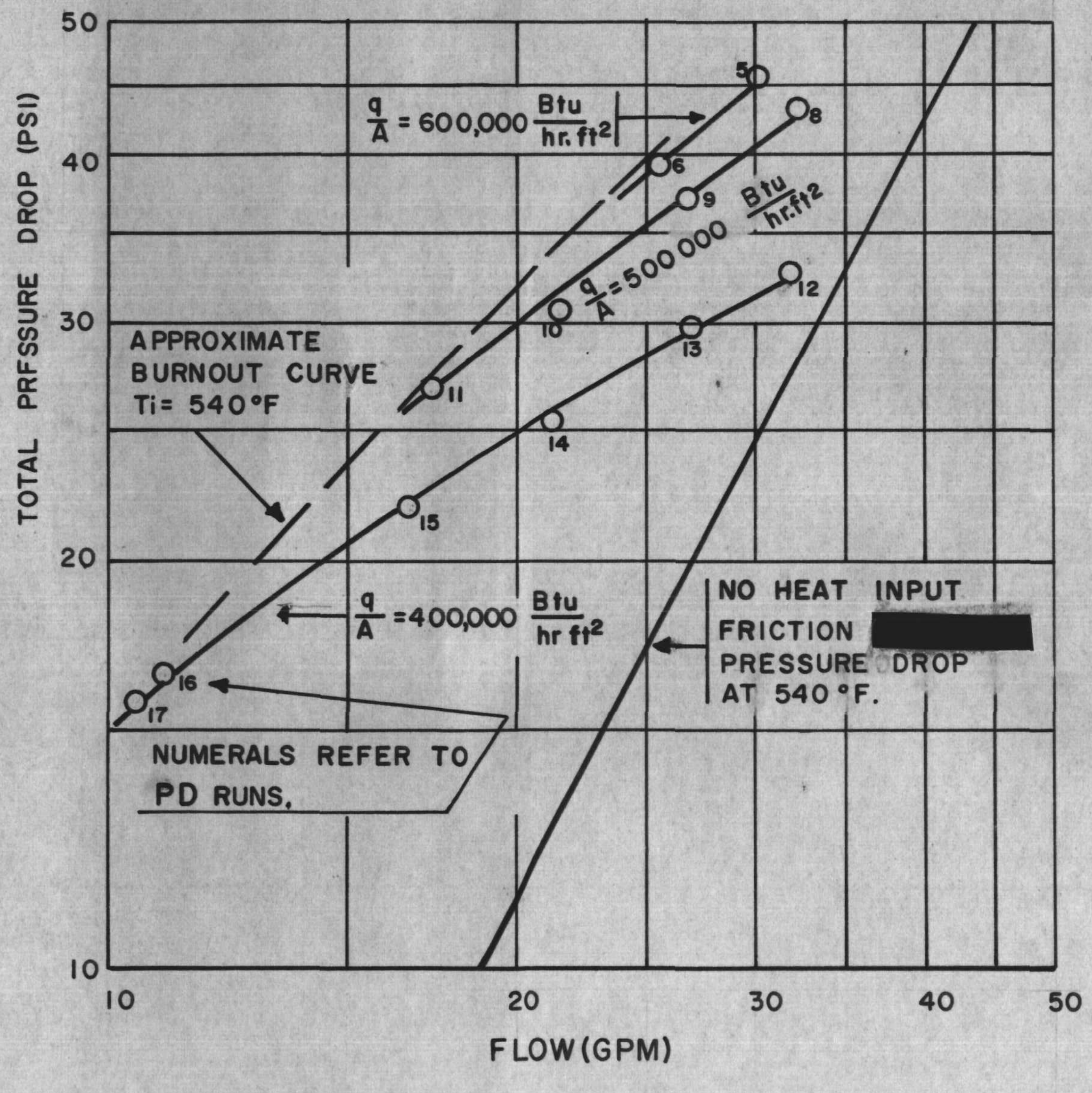

Figure 5

TABLE 1

EXPERIMENTAL RESULTS FOR THE SECOND 12-ROD TEST SECTION

RUN NO.	INLET TEMP (°F)	POWER INPUT (KW)	MASS FLOW RATE (10^6 lb/hr-ft²)	ROD HEAT FLUX (10^6 Btu/hr-ft²)	EXIT QUALITY (%)	BURNOUT INDICATOR
22	387	0.181	0.49	0.310	28.8	T.C. Rod # 4
23	426	0.180	0.50	0.308	33.8	B.O. Detector Rod # 4 T.C. Rod # 4 (runs 23–25)
24	470	0.171	0.51	0.293	38.8	
25	518	0.166	0.48	0.284	48.3	
26	567	0.157	0.51	0.269	52.7	T.C. Rod # 4
27	555	0.229	0.99	0.391	36.6	B.O. Detector Rod # 4 T.C. Rod # 4 (runs 27–28)
28	512	0.266	1.01	0.455	33.5	
29	474	0.283	1.06	0.485	27.0	T.C. Rod # 4
30	427	0.295	0.99	0.504	23.4	B.O. Detector Rod # 4
31	383	0.306	1.02	0.524	16.2	B.O. Detector Rods # 4,3&10
32	323	0.310	0.99	0.530	8.2	B.O. Detector Rod # 4 T.C. Rod # 4
33	374	0.403	1.99	0.690	- 1.9	Indication Unreliable
34	420	0.448	1.91	0.766	11.4	T.C. Rod # 4
35	472	0.430	1.95	0.736	18.6	B.O. Detector Rod # 4 T.C. Rod # 4

TABLE 1

EXPERIMENTAL RESULTS FOR THE SECOND 12-ROD TEST SECTION

(Continued)

RUN NO.	INLET TEMP (°F)	POWER INPUT (KW)	MASS FLOW RATE (10^6 lb/hr-ft^2)	ROD HEAT FLUX (10^6 Btu/hr-ft^2)	EXIT QUALITY (%)	BURNOUT INDICATOR
36	497	0.409	2.03	0.700	20.0	B.O. Detector Rod # 4 T.C. Rods # 4 & 2
37	525	0.355	2.06	0.607	20.5	T.C. Rod # 4
38	550	0.293	2.00	0.502	21.4	B.O. Detector Rod # 4 T.C. Rod # 4
39	545	0.358	3.00	0.612	15.6	T.C. Rod # 4
40	498	0.385	2.00	0.658	18.8	B.O. Detector Rod # 4 T.C. Rod # 4
41	472	0.429	2.03	0.734	17.0	B.O. Detector Rods # 3 & 4 T.C. Rod # 4
42	520	0.409	2.88	0.700	14.5	B.O. Detector Rod # 4 T.C. Rod # 4
43	482	0.503	2.96	0.860	11.7	B.O. Detector Rods # 3 & 4
44	436	0.543	3.02	0.929	5.1	B.O. Detector Rod # 4 T.C. Rod # 4 (runs 44 and 45)
45	417	0.554	2.92	0.948	3.4	
46	462	0.520	2.93	0.889	9.3	T.C. Rod # 4
47	506	0.452	2.92	0.773	13.5	B.O. Detector Rods 3 & 4 T.C. Rod # 4

TABLE 1

EXPERIMENTAL RESULTS FOR THE SECOND 12-ROD TEST SECTION

(Continued)

RUN NO.	INLET TEMP (°F)	POWER INPUT (KW)	MASS FLOW RATE (10^6 lb/hr-ft^2)	ROD HEAT FLUX (10^6 Btu/hr-ft^2)	EXIT QUALITY (%)	BURNOUT INDICATOR
48	533	0.398	2.99	0.680	15.5	B.O. Detector Rod # 4 T.C. Rod # 4
49	218	0.197	0.52	0.336	1.8	T.C. Rod # 4
50	371	0.428	2.05	0.732	- 1.4	Indication Unreliable
51	387	0.468	1.99	0.801	5.8	T.C. Rod # 4
52	469	0.600	4.00	1.025	6.1	B.O. Detector Rod # 4 T.C. Rod # 4
53	486	0.562	3.74	0.962	9.4	B.O. Detector Rod # 4 T.C. Rod # 4
54	506	0.535	3.80	0.915	11.3	T.C. Rod # 2
55	517	0.497	3.70	0.850	12.5	B.O. Detector Rods # 3 & 4 T.C. Rod # 4
56	527	0.457	3.65	0.781	13.0	B.O. Detector Rod # 4 T.C. Rod # 4 (runs 56 and 57)
57	545	0.406	3.44	0.695	15.4	
58	491	0.550	3.56	0.941	10.8	B.O. Detector Rod # 3 T.C. Rod # 2
59	436	0.687	4.00	1.175	3.6	B.O. Detector Rod # 4 T.C. Rod # 4

TABLE 1

EXPERIMENTAL RESULTS FOR THE SECOND 12-ROD TEST SECTION

(Continued)

RUN NO.	INLET TEMP (°F)	POWER INPUT (KW)	MASS FLOW RATE (10^6 lb/hr-ft^2)	ROD HEAT FLUX (10^6 Btu/hr-ft^2)	EXIT QUALITY (%)	BURNOUT INDICATOR
60	409	0.749	4.09	1.280	0.7	T.C. Rod # 4
61	436	0.560	3.00	0.958	6.1	T.C. Rod # 4
62	495	0.478	2.97	0.818	12.8	T.C. Rod # 2
63	539	0.383	2.99	0.655	16.0	T.C. Rod # 4
64	535	0.424	3.52	0.724	13.7	T.C. Rod # 4
65	529	0.327	2.03	0.559	19.6	T.C. Rod # 4

TABLE 2

DATA FOR OPERATION PAST THE INSTRUMENTED BURNOUT POINT WITH THE SECOND 12-ROD T. S.

RUN NO.	INLET TEMP (°F)	POWER INPUT (MW)	MASS FLOW RATE (10^6 lb/hr-ft^2)	ROD HEAT FLUX (10^6 Btu/hr-ft^2)	EXIT QUALITY (%)	MAXIMUM ROD OUTER SURFACE TEMP (°F)	HOT ROD NO.
61	436	0.560	3.00	0.958	6.1	606	4
61-1	436	0.566	3.19	0.968	6.6	692	4
62	495	0.478	2.97	0.818	12.8	615	2
62-1	496	0.488	3.00	0.835	13.3	686	4
63	539	0.383	2.99	0.655	16.0	607	4
63-1	543	0.389	2.99	0.665	16.3	692	4
64	535	0.424	3.52	0.724	13.7	617	4
64-1	537	0.424	3.50	0.726	14.3	689	4
65	529	0.327	2.03	0.559	19.6	597	4
65-1	533	0.328	2.02	0.561	20.7	690	4

Note:

All rod temperatures listed were obtained from thermocouples located at a distance of 1/2" from the downstream end of the heated length.

TABLE 3

NON-BURNOUT RUNS FOR THE SECOND 12-ROD TEST SECTION

RUN NO.	INLET TEMP (°F)	POWER INPUT (MW)	MASS FLOW RATE (10^6 lb/hr.ft^2)	ROD HEAT FLUX (10^6 Btu/hr.ft^2)	EXIT QUALITY (%)
P.D. 1	478	0.416	2.99	0.711	5.8
P.D. 2	469	0.559	4.02	0.956	4.1
P.D. 3	435	0.614	3.83	1.049	0.9
P.D. 4	540	0.369	3.01	0.632	15.2
P.D. 5	535	0.349	3.53	0.596	10.1
P.D. 6	537	0.347	2.98	0.593	13.4
P.D. 7	535	0.300	2.59	0.513	13.0
P.D. 8	539	0.293	3.72	0.500	7.4
P.D. 9	538	0.295	3.12	0.504	9.9
P.D. 10	540	0.296	2.53	0.507	14.0
P.D. 11	542	0.293	2.02	0.500	19.3
P.D. 12	536	0.235	3.71	0.402	4.2
P.D. 13	538	0.235	3.12	0.402	6.8
P.D. 14	541	0.235	2.48	0.402	10.5
P.D. 15	543	0.237	1.93	0.405	15.9
P.D. 16	545	0.237	1.27	0.405	27.0
P.D. 17	544	0.236	1.20	0.404	28.6

TABLE 4

PRESSURE DROP DATA - 12 ROD TEST SECTION NO. 2

UNITS - ΔP;PSI

RUN	ΔP_{1-2}	ΔP_{2-3}	ΔP_{3-4}	ΔP_{4-5}	ΔP_{5-6}	ΔP_{6-7}	ΔP_{7-8}	ΔP_{1-8}
PD 1	4.72	2.24	3.70	3.50	7.30	1.94	1.71	25.50
PD 2	7.95	3.58	5.80	4.90	10.70	2.53	2.37	37.83*
PD 3	7.82	3.40	5.40	4.40	9.50	2.06	1.78	34.36*
PD 4	6.27	3.41	7.90	6.90	11.50	3.10	2.81	41.89*
PD 5	7.16	4.49	8.10	6.90	12.30	3.35	2.89	45.19*
PD 6	5.75	4.31	7.20	6.30	10.50	2.85	2.03	38.94*
PD 7	-	-	-	-	-	2.46	2.28	
PD 8	7.84	4.06	7.30	6.30	11.50	3.12	2.82	42.94*
PD 9	5.70	3.69	6.50	5.70	9.80	2.73	2.39	36.51*
PD 10	4.38	3.28	5.50	4.90	8.10	2.28	2.05	30.49*
PD 11	3.74	3.15	4.90	4.40	6.90	1.89	1.71	26.69*
PD 12	7.04	3.33	5.10	4.10	8.30	2.39	2.26	32.52*
PD 13	5.47	2.94	5.10	4.30	7.70	2.23	2.01	29.75*
PD 14	3.90	2.71	4.60	4.00	6.60	1.89	1.71	25.41*

RUN	ΔP_{1-3}	ΔP_{3-5}	ΔP_{5-7}		
PD 15	5.67	7.48	7.26	1.54	21.95*
PD 16	4.35	5.75	5.26	1.13	16.49*
PD 17	-	-	-		15.72

See attached notes.

TABLE 4

PRESSURE DROP DATA - 12-ROD TEST SECTION NO. 2

(Continued)

1. Distances from inlet of heated length for pressure taps 1 through 8 are 0, 5, 8, 11, 14, 17, 18 1/2, and 20 inches respectively.

2. All ΔP measurements have been corrected to show the difference in pressure readings if two gauges were inserted at the indicated levels.

* By addition.

TABLE 5

OUTSIDE WALL TEMPERATURES AND APPARENT HEAT TRANSFER COEFFICIENTS

Units: T_{wall} (°F); h(Btu/hr-ft² °F)

RUN NO.	ROD #2		ROD #4		ROD #5		ROD #7		ROD #9		ROD #11	
	T_{wall}	h	T_{wall}	h	T_{wall}	h	T_{wall}	h	T_{wall}	h	T_{wall}	h
22	586	16,300	608+	7,550	602	8,850	591	12,900	586	16,300	587	15,500
23	586	16,100	594+	11,300	584	18,000	589	13,900	580*	23,400#	590	13,300
24	587	14,900	600+	8,980	584	17,600	589	13,500	581*	21,500#	589	13,500
25	584	16,800	595+	10,200	581	20,400	587	14,300	578*	27,300#	587	14,300
26	585	15,400	601+	8,050	576	31,900	585	15,400	577*	28,500#	585	15,400
27	587	19,300	591+	16,100	584	22,700	589	17,600	575*	47,600#	587	19,300
28	587	22,800	600+	13,800	585	25,300	590	19,800	580#	35,000#	588	21,700
29	590	21,100	600+	14,700	588	23,100	593	18,700	579#	40,500#	593	18,700
30	590	21,600	583	30,900	589	22,600	595	17,800	579#	41,000#	592	19,900
31	592	21,300	586	28,100	592	21,300	593	20,400	579#	45,100#	595	18,900
32	592	21,700	595+	19,400	592	21,700	580	42,800	579#	46,600#	596	18,700
33	599	21,700	593	25,700	594	24,800	599	21,000	586#	34,800#	598	21,700
34	594	28,100	603+	21,100	596	26,200	599	23,800	587	37,900	583	47,200
35	589	33,100	599+	22,800	594	27,000	597	24,300	594	27,000	594	27,000
36	605+	18,600	614+	15,000	593	27,400	597	23,700	593	27,400	596	24,500
37	586	32,400	654+	7,000	589	28,000	594	22,700	591	25,600	593	23,600
38	590	22,400	609+	12,100	589	23,500	594	19,000	590	12,100	593	19,800
39	593	24,000	593+	24,000	593	24,000	599	19,400	593	24,000	596	21,400
40	590	28,700	613+	14,300	591	27,500	591	27,500	594	24,400	595	23,560
41	592	30,200	595+	26,900	595	26,900	593	29,000	597	25,000	599	23,400
42	593	27,400	592+	28,500	593	27,400	593	27,400	595	25,400	596	24,500
43	596	29,700	594	31,900	597	28,700	595	30,800	598	27,800	600	26,100
44	596	32,500	601+	27,700	598	30,400	597	31,400	600	28,500	601	27,700
45	598	31,700	606+	24,400	600	28,800	597	31,700	600	28,000	603	26,400
46	595	31,800	610+	20,700	601	26,200	594	33,000	598	28,700	599	27,800
47	602	22,400	598+	24,900	595	27,600	590	33,600	596	26,600	596	26,600

TABLE 5 (cont'd)

OUTSIDE WALL TEMPERATURES AND APPARENT HEAT TRANSFER COEFFICIENTS

Units: T_{wall} (°F); h(Btu/hr-ft² °F)

RUN NO.	ROD #2 T_{wall}	ROD #2 h	ROD #4 T_{wall}	ROD #4 h	ROD #5 T_{wall}	ROD #5 h	ROD #7 T_{wall}	ROD #7 h	ROD #9 T_{wall}	ROD #9 h	ROD #11 T_{wall}	ROD #11 h
48	591	28,100	604+	18,300	592	27,000	588	32,100	593	26,000	593	26,000
49	591	[illegible]	>733+	<2,020	589	15,200	589	15,200	589	15,200	589	15,200
50	598	24,100	605	19,600	595	26,700	595	26,700	597	24,900	597	24,900
51	598	25,800	598+	25,800	595	28,600	595	28,600	596	27,600	598	25,800
52	597	34,000	604+	27,600	603	28,300	602	29,100	600	30,900	601	30,000
53	596	33,800	607+	24,400	599	30,600	597	32,700	597	32,700	600	29,600
54	603+	25,400	592	36,500	596	31,500	595	32,600	595	32,600	597	30,500
55	595	30,100	604+	22,800	594	31,200	592	33,600	592	33,600	597	28,100
56	593	30,400	610+	18,300	593	30,400	592	31,600	595	30,410	593	30,410
57	590	30,800	600+	21,200	590	30,600	589	32,000	590	30,600	592	28,100
58	613+	20,400	601	27,500	597	31,200	596	32,300	597	31,200	598	30,200
59	602	33,500	608+	28,600	602	33,500	601	34,500	602	33,500	600	35,600
60	603	36,200	611+	29,200	603	36,200	602	37,300	603	36,200	602	37,300
61	603	27,000	606+	24,900	603	27,000	600	29,400	597	32,400	600	29,400
61-1	599	30,100	692+	7,740	602	27,500	599	30,100	598	30,100	599	30,100
62	615+	17,800	603	23,100	603	23,100	602	26,000	601	26,900	602	26,000
62-1	646	10,600	687+	6,970	604	22,700	603	23,300	600	25,400	601	24,700
63	593	25,100	607+	16,300	597	21,800	596	22,500	591	27,200	580	50,200
63-1	593	25,900	692+	5,330	597	22,400	596	23,200	591	28,100	593	25,900
64	594	27,200	617+	14,600	595	26,200	597	24,400	592	29,400	595	26,200
64-1	595	26,300	689+	5,970	596	25,400	598	23,700	592	29,500	595	26,300
65	591	23,900	597+	19,000	594	21,200	592	22,900	590	24,900	592	22,900
65-1	591	24,100	690+	4,590	594	21,300	593	22,200	590	25,100	593	22,200

TABLE 5 (cont'd)

OUTSIDE WALL TEMPERATURES AND APPARENT HEAT TRANSFER COEFFICIENTS

Units: T_{wall} (°F); h(Btu/hr-ft² °F)

RUN NO.	ROD #2		ROD #4		ROD #5		ROD #7		ROD #9		ROD #11	
	T_{wall}	h	T_{wall}	h	T_{wall}	h	T_{wall}	h	T_{wall}	h	T_{wall}	h
P.D. 1	592	28,300	586	37,200	594	26,200	592	28,300	595	25,300	597	23,600
2	600	29,300	606	24,700	599	30,200	597	32,300	599	30,200	600	29,300
3	598	34,600	598	34,600	599	33,500	598	34,600	599	33,500	600	32,400
4	592	25,400	592	25,400	597	21,100	595	22,700	590	27,600	576	71,200*
5	589	27,000	591	24,700	591	24,700	589	27,000	591	24,700	592	23,700
6	589	26,700	590	25,500	589	26,700	589	26,700	590	25,500	591	24,500
7	591	21,400	592	20,500	592	20,500	591	21,400	593	19,700	593	19,700
8	587	25,700	587	25,700	587	25,700	587	25,700	588	24,500	589	23,300
9	586	26,300	586	26,300	586	26,300	586	26,300	589	22,700	589	22,700
10	586	26,400	587	25,100	586	26,400	586	26,400	589	22,800	589	22,800
11	587	25,700	587	25,700	588	24,500	587	25,700	590	22,300	590	22,300
12	588	18,400	584	23,900	587	20,300	587	20,300	589	18,400	587	20,300
13	589	19,300	584	23,900	587	20,300	586	21,400	587	20,300	587	20,300
14	587	20,300	585	22,500	587	20,300	587	20,300	589	19,300	588	19,300
15	587	20,500	586	21,600	587	20,500	587	20,500	589	18,600	588	18,600
16	590	17,800	587	20,500	589	17,800	589	17,800	590	17,800	590	17,800
17	590	17,700	586	21,500	588	19,400	587	20,400	589	18,500	590	17,700

Notes:

1. The thermocouples on all rods are located 1/2 inch from the downstream end of the heater tubes.

2. The fluid temperature was assumed to be the saturation temperature for all calculations (567.2°F).

* Questionable

\+ These temperature measurements were used to indicate incipient burnout. They are not necessarily steady state values. In most cases a fast temperature rise was terminated by a power reduction.

> Greater than.

< Less than.

Columbia University — Department Of Chemical Engineering
ENGINEERING RESEARCH LABORATORIES

ERRATA FOR TOPICAL REPORT #1

1. The value for ΔP_{6-7}, in Table 2 was given as 5.27; should be 0.56.

2. Note to Table 3 reads:
   ... from the upstream end of the heater tubes.
   This should read: ... from the downstream end of the heater tubes.